OPEN

Citation: Cell Death and Disease (2014) 5, e1186; doi:10.1038/cddis.2014.161
© 2014 Macmillan Publishers Limited All rights reserved 2041-4889/14
www.nature.com/cddis

Identification and characterization of PDGFRα$^+$ mesenchymal progenitors in human skeletal muscle

A Uezumi*[,1], S Fukada[2], N Yamamoto[3], M Ikemoto-Uezumi[4], M Nakatani[1], M Morita[5], A Yamaguchi[5], H Yamada[5], I Nishino[6], Y Hamada[7] and K Tsuchida[1]

Fatty and fibrous connective tissue formation is a hallmark of diseased skeletal muscle and deteriorates muscle function. We previously identified non-myogenic mesenchymal progenitors that contribute to adipogenesis and fibrogenesis in mouse skeletal muscle. In this study, we report the identification and characterization of a human counterpart to these progenitors. By using PDGFRα as a specific marker, mesenchymal progenitors can be identified in the interstitium and isolated from human skeletal muscle. PDGFRα$^+$ cells represent a cell population distinct from CD56$^+$ myogenic cells, and adipogenic and fibrogenic potentials were highly enriched in the PDGFRα$^+$ population. Activation of PDGFRα stimulates proliferation of PDGFRα$^+$ cells through PI3K-Akt and MEK2-MAPK signaling pathways, and aberrant accumulation of PDGFRα$^+$ cells was conspicuous in muscles of patients with both genetic and non-genetic muscle diseases. Our results revealed the pathological relevance of PDGFRα$^+$ mesenchymal progenitors to human muscle diseases and provide a basis for developing therapeutic strategy to treat muscle diseases.

Cell Death and Disease (2014) **5,** e1186; doi:10.1038/cddis.2014.161; published online 17 April 2014
Subject Category: Experimental Medicine

Adult skeletal muscle has remarkable ability to regenerate following muscle damage. This regenerative capacity is attributed to satellite cells, which reside adjacent to and beneath the basal lamina of myofibers. In response to various regenerative stimuli, satellite cells rapidly become activated and proliferate, and then differentiate and fuse with each other or with pre-existing myofibers to regenerate damaged muscle.[1] Satellite cells have been shown to be the major contributor to adult myogenesis,[2–4] and several studies have demonstrated that a subset of satellite cells can self-renew in addition to contributing to differentiated progeny, and thus established their status as adult myogenic stem cells.[5–8]

Despite this exquisite regeneration system, the skeletal muscle is occupied by fatty and fibrous tissue in several pathological conditions such as Duchenne muscular dystrophy (DMD). Because the occurrence of fatty and fibrous tissue is usually associated with loss or extreme atrophy of muscle, the idea that dysregulation of the fate-switch between muscle and nonmuscle lineages in satellite cells may underlie this pathological change has emerged. However, recent studies revealed the presence of mesenchymal progenitors that directly participate in fat infiltration and fibrosis by differentiating into adipocytes or fibroblasts.[9–11] These mesenchymal progenitors specifically express PDGFRα and reside in the interstitial spaces of muscle tissue, and therefore represent a cell population distinct from satellite cells.[9] Furthermore, a lineage-tracing study using MyoD-Cre;R26R-EYFP mice, in which essentially all satellite cells are permanently labeled by a reporter protein, demonstrated that satellite cells are committed to the myogenic lineage and do not spontaneously adopt nonmyogenic fates.[12] These results indicate that regulation of the differentiation pathway in mesenchymal progenitors, not dysregulated differentiation of satellite cells, significantly affects the pathogenesis of skeletal muscle. Therefore, identification of cells equivalent to these mesenchymal progenitors in humans has considerable clinical implication.

Several studies reported the identification of satellite cells in human skeletal muscle. M-cadherin and Pax7 are reliable markers for mouse satellite cells[13,14] and were also used for human satellite cell identification.[15–18] Although CD56 is not expressed by quiescent satellite cells and begins to be expressed only after denervation or differentiation in the mouse,[13,19] both quiescent and activated human satellite cells express CD56, and therefore this molecule has been extensively used as a marker for identification and isolation of satellite cells from human muscle.[20–29]

[1]Division for Therapies against Intractable Diseases, Institute for Comprehensive Medical Science, Fujita Health University, 1-98 Dengakugakubo, Kutsukake, Toyoake, Aichi 470-1192, Japan; [2]Department of Immunology, Graduate School of Pharmaceutical Sciences, Osaka University, 1-6 Yamada-oka, Suita, Osaka 565-0871, Japan; [3]Laboratory of Molecular Biology and Histochemistry, Fujita Health University, Aichi, Japan; [4]Department of Regenerative Medicine, National Institute for Longevity Sciences, National Center for Geriatrics and Gerontology, 35 Gengo, Morioka, Obu, Aichi 474-8511, Japan; [5]Department of Orthopaedic Surgery, Fujita Health University, Aichi, Japan; [6]Department of Neuromuscular Research, National Institute of Neuroscience, National Center of Neurology and Psychiatry, 4-1-1 Ogawa-higashi, Kodaira, Tokyo 187-8502, Japan and [7]Department of Orthopedics, Tokushima Prefectural Central Hospital, 1-10-3 Kuramoto, Tokushima 770-8539, Japan
*Corresponding author: A Uezumi, Division for Therapies against Intractable Diseases, Institute for Comprehensive Medical Science, Fujita Health University, 1-98 Dengakugakubo, Kutsukake, Toyoake, Aichi 470-1192, Japan. Tel: +81 562 93 9393; Fax: +81 562 93 5791; E-mail: uezumi@fujita-hu.ac.jp
Keywords: mesenchymal progenitors; PDGFRα; human muscle; adipogenesis; fibrosis
Abbreviations: PDGFRα, platelet-derived growth factor receptor-α; DMD, Duchenne muscular dystrophy; FACS, fluorescence-activated cell sorting; TGF-β, transforming growth factor-β
Received 17.10.13; revised 03.3.14; accepted 04.3.14; Edited by M Federici

Cells with adipogenic potential have also been isolated from human skeletal muscle. These cells were isolated using CD34[26,30] or CD15[27,28] as markers. However, both markers are expressed on many different cell types, including myeloid cells of hematopoietic lineage. CD34 is expressed on early precursor cells of myeloid and B-cell lineages, and CD15 is expressed on immature monocytic lineage cells and highly expressed on granulocytic lineage cells.[31] As diseased muscle contains many myeloid cells such as neutrophils, monocytes, and macrophages, a more specific marker for mesenchymal cells with adipogenic potential is required for detailed characterization of these cells in human diseased muscle.

In this study, we use PDGFRα, which has been shown to indicate specifically mesenchymal progenitors in mouse skeletal muscle,[9] as a marker to isolate and characterize human counterpart to these cells. Our results revealed the pathological relevance of PDGFRα$^+$ mesenchymal progenitors to human muscle diseases.

Results

Localization of PDGFRα$^+$ cells in human skeletal muscle. We previously identified PDGFRα$^+$ cells in the interstitial space of mouse skeletal muscle and showed that these cells represent a unique mesenchymal progenitor population distinct from satellite cells.[9] Because PDGFRα$^+$ mesenchymal progenitors have been demonstrated to contribute to pathologic changes of skeletal muscle such as fatty degeneration and fibrosis in a mouse model,[9,10] it is clinically important to characterize such cells in humans. Therefore, we analyzed human skeletal muscle using PDGFRα as a marker for mesenchymal progenitors. We first identified satellite cells on human muscle sections. M-cadherin,[15] Pax7[16–18,32] and CD56[20–22,32] have been used as markers for human satellite cell identification, but it was also reported that basal lamina staining was necessary for reliable detection of human satellite cells.[18] When human muscle sections were stained with antibodies against M-cadherin, Pax7 and laminin, M-cadherin$^+$Pax7$^+$ satellite cells locating beneath the basal lamina were identified (Figure 1a). We observed 434 M-cadherin$^+$ sublaminar satellite cells on muscle sections from 10 different patients, and found 99.5% of them were also positive for CD56 (Figure 1b). Thus, these markers in combination with basal lamina staining were useful for the identification of human satellite cells. We next examined the relationship between satellite cells and PDGFRα$^+$ cells. PDGFRα$^+$ cells were found in the interstitial space of human muscle, whereas satellite cells (stained with Pax7 or CD56 antibody) were localized beneath the basal lamina, as described above (Figures 1c and d). We carefully examined muscle sections from 24 different patients, but never observed PDGFRα$^+$ cells that satisfy the criteria for satellite cells (markers and localization). These results indicate that PDGFRα$^+$ cells and satellite cells represent discrete cell populations in humans, similar to the results obtained from mice.[9] PDGFRα$^+$ cells were more frequently observed in the perimysium than in the endomysium and were conspicuous in the perivascular space (Figure 1e).

Isolation of PDGFRα$^+$ cells from human skeletal muscle. We next sought to isolate PDGFRα$^+$ cells from human muscle. Because the starting volume of human muscle obtained from biopsy was limited (typically 0.1–0.3 g), we enzymatically digested human muscle and first cultured dissociated cells. Because human muscle-derived cells grew vigorously in a hypoxic condition (3% O_2) compared with a normoxic condition (see Supplementary Figure S1), we used the hypoxic condition to expand or maintain the cells in the following experiments. However, cells in a normoxic condition showed more efficient differentiation (data not shown), and therefore a normoxic condition was used in differentiation experiments. When cells reached ~70% confluence, human muscle-derived cells were analyzed for PDGFRα and CD56 expression by flow cytometry. Populations positive for these markers were clearly observed in varying percentages in 30 different preparations (PDGFRα$^+$ cells ranging from 10 to 73% and CD56$^+$ cells ranging from 6 to 68%; Figure 2a). Importantly, PDGFRα$^+$ cells and CD56$^+$ cells represented discrete single-positive populations and never overlapped each other. Because CD56$^-$ cells was reported to give rise to CD56$^+$ cells and CD56$^+$ cells lose CD56 expression during long-term culture,[33] we reanalyzed PDGFRα and CD56 expression after two passages (totally, three passages). Almost all PDGFRα$^+$ cells maintained their PDGFRα single-positive state, and so did CD56$^+$ cells in our culture condition (Figures 2c and d). This was also confirmed by immunofluorescent staining of cultured cells (see Supplementary Figure S2). The cell surface phenotype of PDGFRα$^+$ cells differs from that of CD56$^+$ cells in the expression of CD90 and CD166, but is similar to that of bone marrow-derived mesenchymal stromal cells (Figures 2e–g). It has been reported that CD166, also known as ALCAM, is expressed on human bone marrow-derived mesenchymal stem cells.[34] Three-color fluorescence-activated cell sorting (FACS) analysis revealed that CD56$^-$PDGFRα$^+$ cells are almost identical to CD56$^-$CD166$^+$ cells (see Supplementary Figure S3). Therefore, CD166 can be an additional marker to identify mesenchymal progenitors in human muscle.

The three human muscle-derived cell populations were sorted by FACS, and gene expression was examined by RT-PCR. Myogenic genes were detected only in CD56$^+$ cells, indicating that satellite cell-derived myogenic cells were exclusively sorted in this population (Figure 3a). After culturing in the growth condition, the myogenic markers MyoD and Pax7 were again detected only in CD56$^+$ cells, and other populations did not become positive for these markers (Figure 3b).

PDGFRα$^+$ cells efficiently differentiate into adipocytes, but CD56$^+$ cells differentiate into myotubes even under adipogenic differentiation condition. The three human muscle-derived cell populations were induced to differentiate into adipocytes. PDGFRα$^+$ cells efficiently differentiated into adipocytes, adopting a spherical shape, accumulating lipid, and expressing the adipogenic transcription factors C/EBPα and PPARγ (Figure 4a). After adipogenic differentiation, PDGFRα$^+$ cells were no longer positive for PDGFRα (data not shown). CD56$^+$ cells did not show any adipogenic

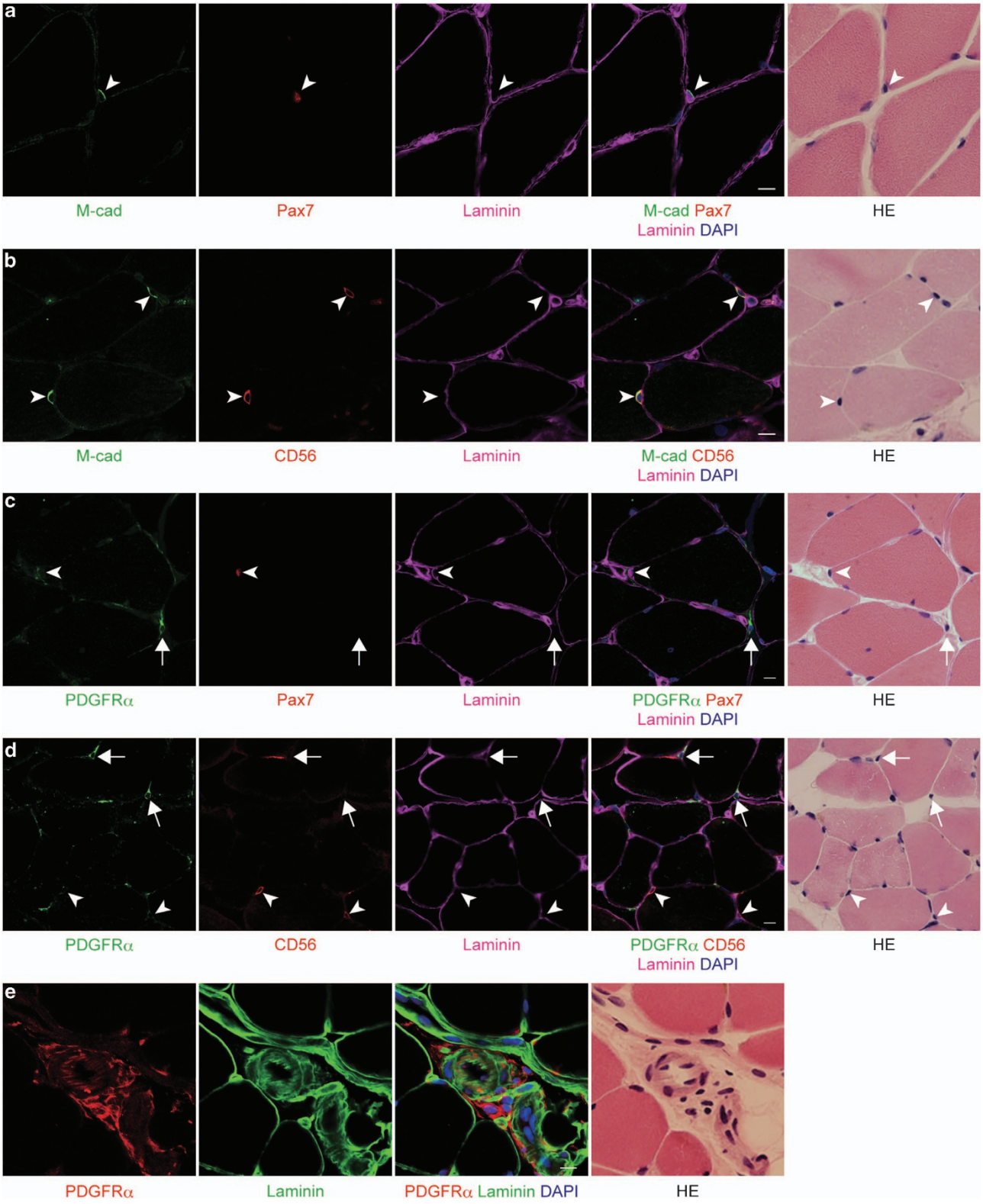

Figure 1 Localization of PDGFRα$^+$ cells in human skeletal muscle. Human muscle sections were stained with antibodies against M-cadherin, Pax7, and laminin (**a**); M-cadherin, CD56, and laminin (**b**); PDGFRα, Pax7, and laminin (**c**); PDGFRα, CD56, and laminin (**d**); and PDGFRα and laminin (**e**), followed by HE staining. Arrows indicate PDGFRα$^+$ cells located in the interstitial spaces of muscle tissue, and arrowheads indicate satellite cells located beneath the basement membrane. Scale bars: 10 μm

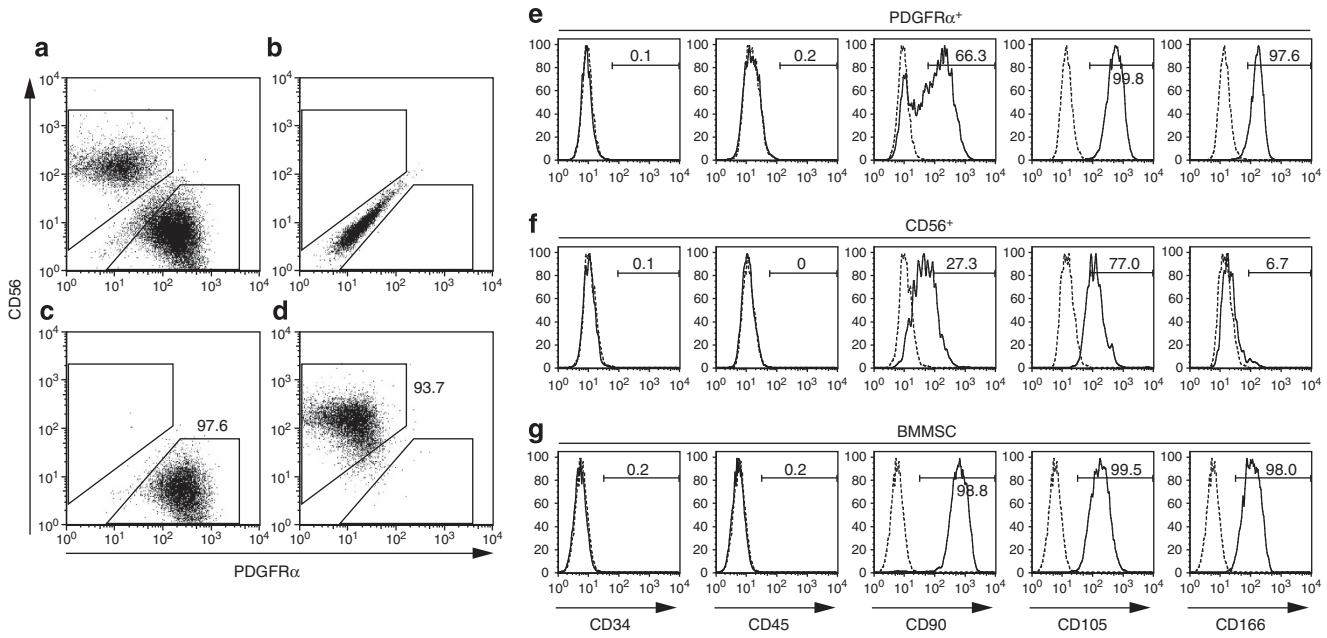

Figure 2 Flow cytometric analysis of PDGFRα^+ cells. (**a**) Human muscle-derived cells were analyzed for PDGFRα and CD56 expression. Representative data of 30 independent experiments are shown. (**b**) Positive gates were set by analyzing negative control samples stained with isotype control antibody or secondary reagent only. (**c**) Sorted PDGFRα^+ cells were reanalyzed for PDGFRα and CD56 expression. Consistent results were obtained from two independent experiments. (**d**) Sorted CD56$^+$ cells were reanalyzed for PDGFRα and CD56 expression. Consistent results were obtained from two independent experiments. Expressions of indicated cell surface antigens, PDGFRα^+ cells (**e**), CD56$^+$ cells (**f**), and bone marrow-derived mesenchymal stem cells (BMMSC, **g**) were analyzed. Positive gates were set by analyzing negative control samples stained with isotype control antibody (dotted line). The percentages of each cell population are shown in the panels

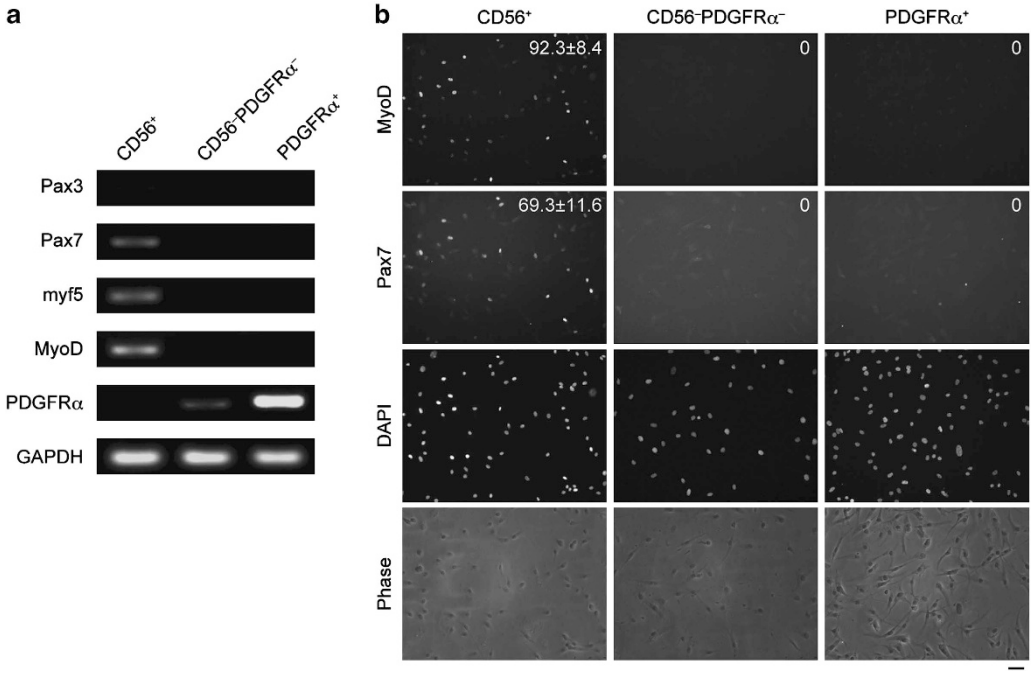

Figure 3 Myogenic markers are detected only in CD56$^+$ population. (**a**) Reverse transcription-polymerase chain reaction (RT-PCR) analysis of indicated genes in the three populations indicated. RNA was extracted immediately after cell sorting, and RT-PCR was performed. (**b**) The three indicated populations were cultured for 3 days in growth conditions after cell sorting and then stained with antibodies against MyoD and Pax7. The percentages of positive cells are shown in the panels as means ± s.d., $n = 20$ fields from three independent preparations. Scale bar: 50 μm

activity, but a few CD56$^-$PDGFRα^- cells differentiated into C/EBPα^+PPARγ^+ adipocytes (Figure 4a). However, PDGFRα^+ cells were stained significantly more by Oil Red O than the other two populations (Figure 4b), indicating that adipogenic differentiation potential is highly enriched in the PDGFRα^+ population of human muscle-derived cells.

PDGFRα$^+$ cell-derived adipocytes express both white and brown adipocyte-specific genes, *Leptin* and *UCP1*, indicating that PDGFRα$^+$ cells possess the capacity to differentiate into both white and brown adipocytes (Figure 4c).

When myogenic differentiation was evaluated after adipogenic induction, we did not see any myogenic activity in PDGFRα$^+$ cells and CD56$^-$PDGFRα$^-$ cells (Figure 4d). However, even on adipogenic induction, CD56$^+$ cells differentiated into large well-developed myotubes expressing myogenic proteins such as MyoD and myosin heavy chain (MyHC) (Figure 4d). In light of the results that CD56$^+$ cells cannot undergo adipogenesis (Figures 4a and b), CD56$^+$ cells appear to be committed to a myogenic lineage and cannot convert their fate into other lineages.

Fibrogenic potential of PDGFRα$^+$ cells and effects of TGF-β and PDGF signaling on PDGFRα$^+$ cells. In the mouse, PDGFRα$^+$ cells not only differentiate into adipocytes but also produce fibrogenic cells and contribute to fibrosis of the skeletal muscle.[9–11] We therefore investigated the fibrogenic property of human muscle-derived PDGFRα$^+$ cells. We performed clonal culture and found that 71 out of 576 PDGFRα$^+$ cells formed colonies and that 29.6% of these colonies were adipogenic. Interestingly, all adipogenic colonies consisted not only of adipocytes but always contained collagen I or α-smooth muscle actin-expressing fibrogenic cells (Figure 5a). These results suggest that a single human muscle-derived PDGFRα$^+$ cell can produce both adipocytes and fibrogenic cells.

Transforming growth factor-β1 (TGF-β1) is known as potent profibrogenic cytokine, and we previously reported that this cytokine induces the expression of fibrosis markers in mouse PDGFRα$^+$ cells.[10] Human muscle-derived PDGFRα$^+$ cells expressed much higher levels of fibrosis-related molecules compared with CD56$^+$ cells, and these expressions were further upregulated in response to TGF-β1 stimulation (Figures 5b and c). TGF-β1 treatment did not affect MMP activity and TIMP-1 expression (Figures 5d and e), suggesting that upregulation of collagens and α-SMA does not merely reflect an increase in remodeling. These results suggest the possibility that fibrosis observed in human skeletal muscle is mainly attributable to PDGFRα$^+$ cells rather than CD56$^+$ myogenic cells.

Constitutively active PDGFRα knock-in mice displayed connective tissue hyperplasia and developed systemic fibrosis including the skeletal muscle,[35] and stimulation of PDGFRα signaling promoted proliferation of mouse PDGFRα$^+$ cells.[10] These reports prompted us to examine the effect of PDGF-PDGFRα signaling on human muscle-derived PDGFRα$^+$ cells. Addition of PDGF-AA to serum-free medium (SFM) activated PDGFRα on human PDGFRα$^+$ cells, and this activation was inhibited by imatinib, a tyrosine kinase inhibitor, or by a specific neutralizing antibody (Figure 5f). The effect of PDGFRα signaling on the proliferation of PDGFRα$^+$ cells was evaluated by measuring 5-bromo-2′-deoxyuridine (BrdU) incorporation. PDGFRα stimulation promoted the proliferation of PDGFRα$^+$ cells, and imatinib or neutralizing antibody completely inhibited this growth-stimulating activity (Figure 5g). To further investigate the signaling pathway through which PDGFRα promotes the proliferation of PDGFRα$^+$ cells, we used inhibitors of PI3K-Akt and Ras-MAPK pathways, which are known to be downstream signaling pathways of PDGFRα.[36] The inhibitors did not affect the viability of PDGFRα$^+$ cells *per se* at the concentrations used in these experiments (see Supplementary Figure S4). LY294002 (PI3K inhibitor) and U0126 (MEK1/2 inhibitor) completely inhibited the stimulatory effect of PDGF-AA, but PD98059 (MEK1 inhibitor) had no effect (Figure 5g), suggesting that PDGFRα exerts its proliferative effect through PI3K-Akt and MEK2-MAPK pathways. LY294002 strongly inhibited Akt phosphorylation induced by PDGF-AA but had no effect on MAPK activation, whereas U0126 strongly inhibited p44/42 MAPK phosphorylation induced by PDGF-AA but had no effect on Akt activation (Figures 5h and i). Thus, both PI3K-Akt and MEK2-MAPK pathways are necessary for PDGFRα-driven proliferation.

Behavior of PDGFRα$^+$ cells in diseased human muscle. To establish the clinical relevance of PDGFRα$^+$ cells, we examined skeletal muscles of DMD patients. In DMD, dystrophin deficiency evokes repeated regeneration–degeneration cycles and eventually leads to the development of fatty and fibrous connective tissue in the skeletal muscle. Many PDGFRα$^+$ cells were observed around ectopically formed fat cells in DMD muscles (Figure 6a). Although fat cells themselves were negative for PDGFRα, we found some PDGFRα$^+$ cells expressing PPARγ in proximity to perilipin$^+$ ectopic fat cells (Figure 6b). When we looked at fibrotic areas of DMD muscles, a striking increase in the number of PDGFRα$^+$ cells coincided with increased fibrosis (Figure 6c). Considerable accumulation of PDGFRα$^+$ cells was prominent, particularly around blood vessels, but they never overlap with vascular components such as endothelial cells or mural cells (Figures 6d and e). Such aberrant behavior of PDGFRα$^+$ cells was observed in all the patients we investigated. In contrast to PDGFRα$^+$ cells, CD56$^+$ cells were not observed around ectopic fat and in fibrotic areas where many PDGFRα$^+$ cells were localized, but they were located on the inside of the basal lamina (Figure 6f). We next investigated skeletal muscles of a patient who suffered from Volkmann's contracture. Volkmann's contracture is caused by acute ischemia and necrosis of the muscles of the forearm and results in fatty and fibrous degeneration of affected muscles. Thus, this condition represents a non-genetic disorder of skeletal muscle. We found severe fatty and fibrous degeneration with the increased number of PDGFRα$^+$ cells in the patient's muscle (Figure 6g).

We next explored the relation between the extent of PDGFRα staining and severity of fibrosis. Muscles from 11 DMD patients with a range of symptoms and 3 normal muscle samples were analysed. HE staining revealed a broad range of dystrophic phenotype of the patients (Figures 7a–c and Supplementary Figure S5). Muscles with severe dystrophic phenotype typically showed more intense PDGFRα staining (Figures 7d–f and Supplementary Figure S5). Many PDGFRα$^+$ cells were localized to collagen-deposited fibrotic areas in DMD muscles, but only a few PDGFRα$^+$ cells could be encountered in the interstitial space of normal muscles where weak collagen expression was observed (Figures 7d–f and Supplementary Figure S5). The extent of PDGFRα

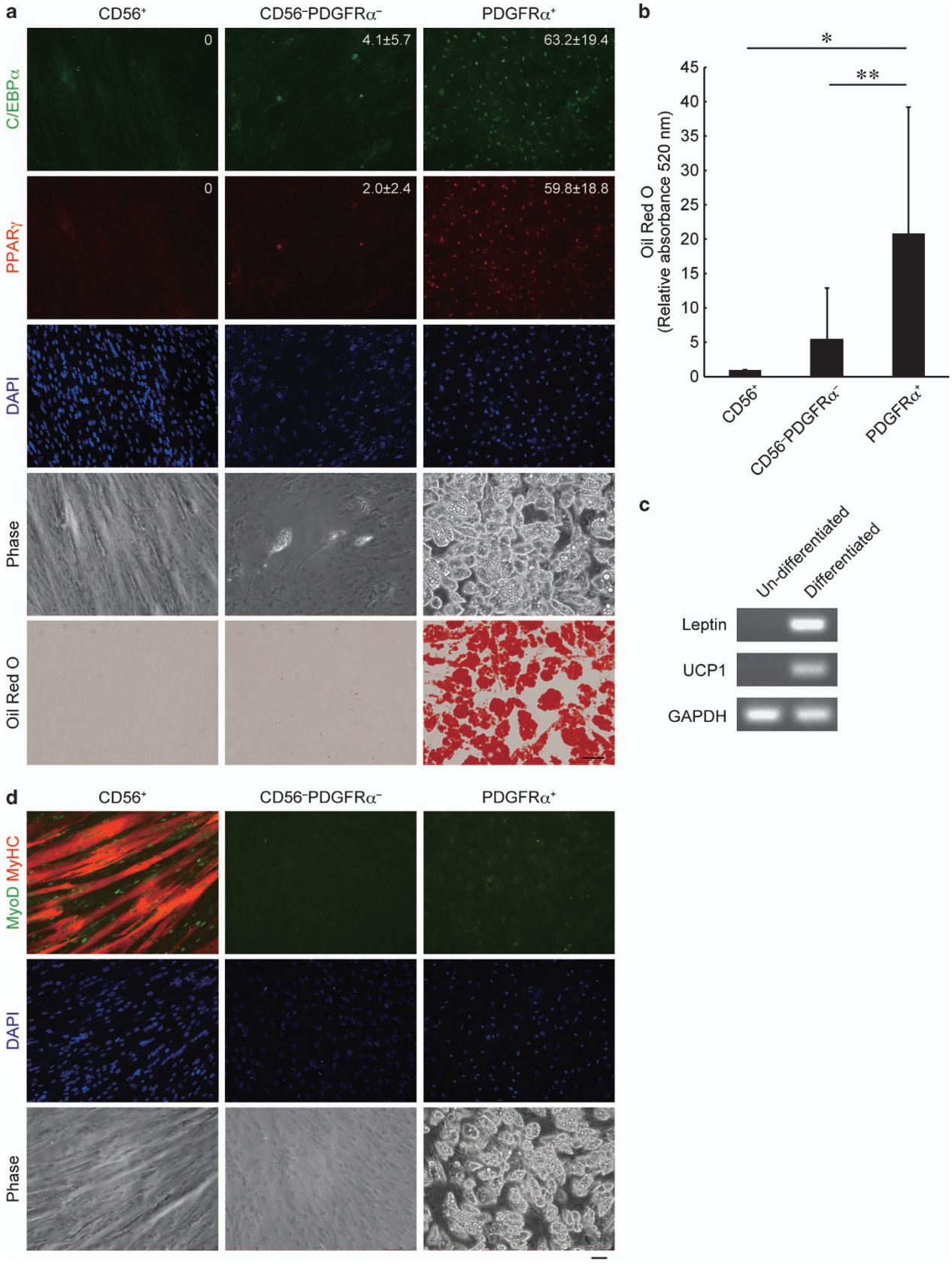
a
CD56+
CD56-PDGFRα-
PDGFRα+
C/EBPα
PPARγ
DAPI
Phase
Oil Red O
0
4.1±5.7
63.2±19.4
0
2.0±2.4
59.8±18.8
b
Oil Red O
(Relative absorbance 520 nm)
45
40
35
30
25
20
15
10
5
0
*
**
CD56+
CD56-PDGFRα-
PDGFRα+
c
Un-differentiated
Differentiated
Leptin
UCP1
GAPDH
d
CD56+
CD56-PDGFRα-
PDGFRα+
MyoD MyHC
DAPI
Phase

staining was graded on a scale of 1–5 (grade 1 represents muscles with occasional PDGFRα$^+$ cells in the interstitium and grade 5 represents muscles with numerous PDGFRα$^+$ cells in the extended interstitial space, see Supplementary Figure S5), and the degree of fibrosis was quantified by measuring hydroxyproline (HOP) content.[37] Statistical analysis indicate significant correlation between the extent of PDGFRα staining and severity of fibrosis (Figure 7g). Taken together, these results strongly suggest that PDGFRα$^+$ mesenchymal progenitors are involved in the pathogenesis of human skeletal muscle.

Discussion

Fatty and fibrous degeneration is a hallmark of diseased skeletal muscle and is very prominent in pathological conditions such as muscular dystrophy[38] or aging.[39] Because fatty and fibrous connective tissue lacks contractile ability, it becomes an aggravating factor in muscle weakness. We previously identified mesenchymal progenitors residing in mouse muscle interstitium using PDGFRα as a specific marker and demonstrated that these cells directly contribute to fatty and fibrous connective tissue development in the skeletal muscle.[9,10] A human counterpart to these progenitors would be a therapeutic target for muscle diseases accompanied by fat infiltration and fibrosis. Other groups also identified progenitors with adipogenic potential in mouse skeletal muscle using Sca-1 as a marker.[11,40] However, there is no human ortholog of Sca-1; in fact, a 500-kb region of mouse chromosome 15 encoding several Ly6 family members including Sca-1 was deleted between mouse and rat speciation.[41] Thus, this marker is not applicable to human study. In this study, we used PDGFRα, which is conserved in humans, and demonstrated that cells equivalent to mouse PDGFRα$^+$ mesenchymal progenitors can be identified in human muscle using the same marker. PDGFRα was also used for the prospective isolation of mesenchymal stem cells from murine embryos and bone marrow of adult mice.[42,43] Furthermore, a recent study succeeded in purifying mesenchymal stem cells possessing hematopoietic stem cell niche activity from human bone marrow by using PDGFRα in combination with CD51.[44] Because mesenchymal stem/progenitor cells are reported to exist in almost all organs of both mice and humans,[45,46] it will be interesting to see whether PDGFRα can serve as a universal marker to identify mesenchymal stem/progenitor cells in diverse organs of various species.

Although the functional significance of PDGFRα in development is evident as PDGFRα-null mice die *in utero*,[47] its role in the adult physiological context has not yet been completely understood. However, several studies, including ours, revealed a link between PDGFRα and fibrogenesis. Olson and Soriano[35] generated mice in which mutant PDGFRα with increased kinase activity was knocked into a PDGFRα locus and thus increased PDGFRα signaling is operative only in cells that express PDGFRα endogenously. Importantly, the engineered mice showed progressive fibrosis in multiple organs including the skeletal muscle.[35] A connection between PDGFRα and the pathogenesis of fibrosis has also been revealed by studies using imatinib, an inhibitor of several tyrosine kinases, including PDGFR, c-kit, and bcr-abl oncogene. Imatinib was shown to ameliorate the muscle dystrophy of mdx mice.[48,49] We also showed that imatinib is effective for improving dystrophic symptoms of DBA/2-mdx, a more severe mouse model of muscular dystrophy.[50] Imatinib-treated mdx muscle showed decreased PDGFRα phosphorylation,[48] and treatment of PDGFRα$^+$ mesenchymal progenitors with imatinib resulted in inhibition of PDGFRα-induced proliferation and expression of fibrotic genes,[50] indicating that the therapeutic effect of imatinib was achieved at least in part through targeting PDGFRα$^+$ mesenchymal progenitors. The antifibrotic effect of imatinib associated with inhibition of PDGFRα activity was also seen in a rat model of myocardial fibrosis.[51] In the present study, we showed that imatinib or a specific neutralizing antibody effectively inhibited PDGFRα phosphorylation and proliferation of human PDGFRα$^+$ mesenchymal progenitors. The growth-stimulating activity of PDGFRα depends on both PI3K-Akt and MEK2-MAPK signaling pathways. Importantly, increased accumulation of PDGFRα$^+$ cells was conspicuous in the skeletal muscle of patients with both genetic and non-genetic muscle diseases, whereas this aberrant increase in the number of PDGFRα$^+$ cells was never found in healthy muscle. Consequently, PDGFRα may have great value not merely as a good marker but also as a molecular therapeutic target for muscular disorders associated with fibrosis.

Wosczyna *et al.*[52] demonstrated that Tie2$^+$PDGFRα$^+$ Sca-1$^+$ progenitors are the cellular origin of ectopic bone in a BMP2-induced mouse model of heterotopic ossification (HO).[52] The progenitor cells identified by Wosczyna *et al.*[52] appear identical to the mesenchymal progenitors described by us because both of them are located in the muscle interstitium and showed similar expression profiles of cell surface antigens.[9] We further showed that human muscle-derived PDGFRα$^+$ mesenchymal progenitors formed bone-like tissue after subcutaneous transplantation into immunodeficient mice, and that the number of PDGFRα$^+$ cells was increased in proximity to ectopically formed bone in the muscle of a patient who developed HO.[53] Therefore, it is highly probable that PDGFRα$^+$ mesenchymal progenitors contribute to HO in addition to fatty and fibrous connective tissue formation.

In addition to their roles in pathogenesis of skeletal muscle, PDGFRα$^+$ mesenchymal progenitors have been shown to

Figure 4 Adipogenic differentiation of PDGFRα$^+$ cells and myogenic differentiation of CD56$^+$ cells after adipogenic induction. (**a**) The three populations indicated were sorted from human muscle-derived cells and cultured in growth condition for 3 days, and then cells were subjected to adipogenic condition. Cells were stained with antibodies against C/EBPα and peroxisome proliferator-activated receptor-γ (PPARγ) or Oil Red O. The percentages of positive cells are shown in the panels as means ± s.d., $n = 15$ fields from three independent preparations. Scale bar: 50 μm. (**b**) Adipogenic differentiation was evaluated by quantifying the intensity of Oil Red O staining. Values are represented as the ratio to CD56$^+$ cells and shown as means ± s.d. of eight independent preparations. *$P < 0.01$, **$P < 0.05$. (**c**) Reverse transcription-polymerase chain reaction (RT-PCR) analysis of indicated genes in undifferentiated PDGFRα$^+$ cells and PDGFRα$^+$ cell-derived adipocytes. (**d**) After adipogenic induction, the three populations indicated were stained with antibodies against MyoD and MyHC. Scale bar: 50 μm

regulate positively muscle regeneration in mouse. Joe *et al.*[11] showed that mesenchymal progenitors promote myogenic differentiation of cocultured satellite cells.[11] Their support function in muscle regeneration has also been demonstrated by using genetically engineered mice that permit conditional ablation of Tcf4$^+$ connective tissue fibroblasts.[54]

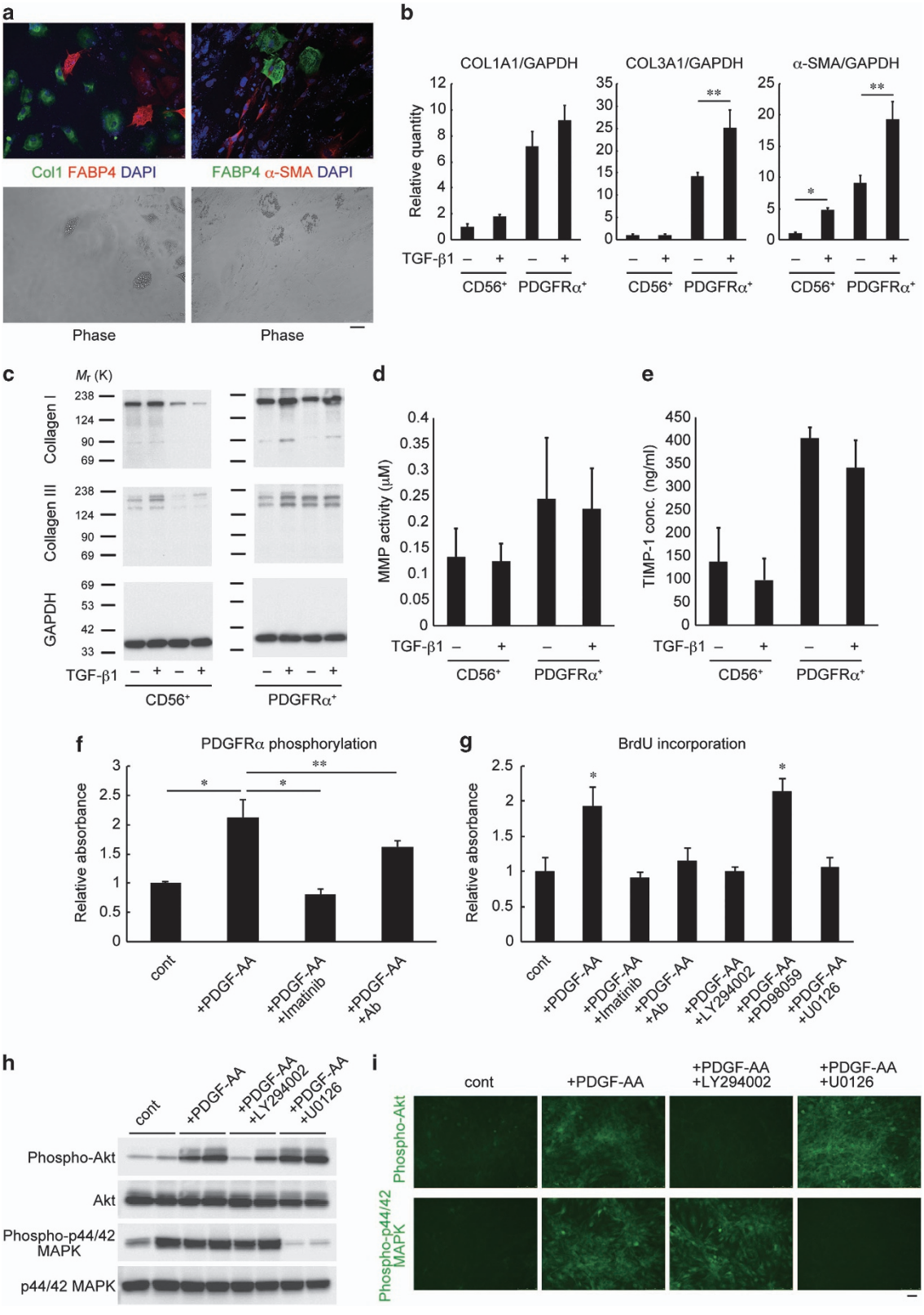

Tcf4$^+$ cell-ablated mice showed impaired muscle regeneration with premature satellite cell differentiation, depletion of the early pool of satellite cells and smaller regenerated myofibers.[54] Although precise relationship between Tcf4$^+$ cells and mesenchymal progenitors remains to be demonstrated, Tcf4$^+$ cells express PDGFRα.[54] Thus, these cells appear to be largely overlapping.

Given the pathophysiological importance of PDGFRα^+ mesenchymal progenitors, isolation of these progenitors from human muscle could be of considerable clinical value. Our method for isolating mesenchymal progenitors is based on the expression of PDGFRα, which is specific and functionally important, and therefore reliable and highly reproducible. Thus, techniques described in this study provide a platform for studying muscle pathophysiology and developing a therapeutic strategy to treat muscle diseases.

Materials and Methods

Human muscle samples. Experiments using human samples were approved by the Ethical Review Board for Clinical Studies at Fujita Health University. Non-dystrophic muscle samples were obtained from gluteus medius muscles of patients undergoing total hip arthroplasty. Muscle samples for histological analysis were obtained from 26 patients ranging in age from 32 to 85 years. Muscle samples for cell culture were obtained from 35 patients ranging in age from 35 to 78 years. DMD muscle samples were obtained from muscle (rectus femoris or biceps brachii) biopsies performed on 16 DMD patients ranging in age from 9 months to 16 years for diagnostic purposes. Dystrophin deficiency was confirmed by immunohistochemistry and western blotting. For Volkmann's contracture muscle samples, forearm muscle tissues were obtained from a 54-year-old patient diagnosed with Volkmann's contracture after trauma to the axillary brachial artery. All patients or their parents gave written informed consent.

Histochemistry, cytochemistry and microscopy. Muscle samples for histochemistry were rapidly frozen in isopentane cooled with liquid nitrogen. Frozen muscle sections (7 μm thick) were cut by cryostat and fixed with 4% paraformaldehyde (PFA) for 5 min. The Volkmann's contracture sample was fixed with 10% formaldehyde, and then embedded in paraffin. Paraffin-embedded sections (5 μm thick) were deparaffinized and treated with Antigen Retrieval Reagent (R&D, Minneapolis, MN, USA). Cultured cells were rinsed with PBS and then fixed with 4% PFA for 5 min. Specimens were blocked with protein-block serum-free reagent (Dako, Glostrup, Denmark) for 15 min, and incubated with primary antibodies at 4 °C overnight, followed by secondary staining. Primary antibodies used were anti-PDGFRα (2.5 μg/ml; R&D; cat. no. AF-307-NA), anti-M-cadherin (1 : 200; R&D), anti-Pax7 (1 : 2; DSHB, Iowa City, IA, USA), anti-CD56 (1 : 20; Miltenyi Biotec, Bergisch Gladbach, Germany), anti-laminin (1 : 200; Sigma, St. Louis, MO, USA), anti-MyoD (1 : 400; Santa Cruz, Dallas, TX, USA), anti-C/EBPα (1 : 400; Santa Cruz), anti-PPARγ (1 : 100; Santa Cruz), anti-MyHC (1 : 2; DSHB), anti-collagen I (1 : 250; Abcam, Cambridge, MA, USA), anti-FABP4 (1 : 50; R&D), anti-α-SMA (1 : 200; Sigma), anti-phospho-Akt (1 : 100; Cell Signaling, Danvers, MA, USA), anti-phospho-p44/42 MAPK (1 : 200; Cell Signaling), and anti-perilipin (1 : 250; Sigma). Secondary antibodies used with a dilution of 1 : 1000 were Alexa Fluor 488- or 568-conjugated anti-goat IgG (Molecular Probes, Carlsbad, CA, USA), CF488A-conjugated anti-sheep IgG (Biotium, Hayward, CA, USA), Cy3-conjugated anti-mouse IgG (Jackson, West Grove, PA, USA), and Alexa Fluor 488- or 647-conjugated anti-rabbit IgG (Molecular Probes). Specimens were counterstained with DAPI (Invitrogen, Carlsbad, CA, USA) and mounted with SlowFade Gold anti-fade reagent (Invitrogen). For sequential immunohistochemistry and HE staining, immunofluorescent staining was performed first and immunofluorescent images were captured. Slides were immersed in PBS to remove the cover glass and subjected to HE staining. Then, images of the corresponding HE-stained fields were captured. To stain lipids, cells were fixed in 10% formalin, rinsed in water, and then 60% isopropanol, stained with Oil Red O in 60% isopropanol, and rinsed in water. Stained cells and tissues were photographed using a fluorescence microscope BX51 (Olympus) equipped with a DP70 CCD camera (Olympus, Tokyo, Japan) or an inverted fluorescence microscope DMI4000B (Leica, Wetzlar, Germany) equipped with a DFC350FX CCD camera (Leica). Confocal images of muscle sections were taken using the confocal laser scanning microscope system LSM700 (Carl Zeiss, Oberkochen, Germany).

Cell preparation. Muscles were transferred to PBS. Nerves, blood vessels, tendons, and fat tissues were carefully removed under a dissection microscope. Trimmed muscles were minced and digested with 0.2% type II collagenase (Worthington, Lakewood, NJ, USA) for 30 min at 37 °C. Digested muscles were passed through an 18 G needle several times and further digested for 10 min at 37 °C. Muscle slurries were filtered through a 100-μm cell strainer (BD Biosciences, Franklin Lakes, NJ, USA) and then through a 40-μm cell strainer (BD Biosciences). Erythrocytes were eliminated by treating the cells with Tris-buffered 0.8% NH_4Cl. Cells were resuspended in the growth medium (GM) consisting of DMEM supplemented with 20% FBS, 1% penicillin–streptomycin, and 2.5 ng/ml bFGF (Invitrogen), and maintained at 37 °C in 5% CO_2 and 3% O_2. Human bone marrow mesenchymal stromal cells (Lonza, Basel, Switzerland) were maintained in DMEM supplemented with 10% FBS and 1% penicillin–streptomycin at 37 °C in 5% CO_2 and 21% O_2.

FACS. Cells were trypsinized and resuspended in washing buffer consisting of PBS with 2.5% FBS, and stained with primary antibodies for 30 min at 4 °C. Cells were then stained with streptavidin-PE/Cy5 (1 : 200; BD Pharmingen, Franklin Lakes, NJ, USA) for 30 min at 4 °C in the dark. Primary antibodies used for cell staining were PE-conjugated anti-CD56 (1 : 20; Miltenyi Biotec), biotinylated anti-PDGFRα (2.5 μg/ml; R&D; cat. no. BAF322), FITC-conjugated anti-CD34 (1 : 10; BD Pharmingen), FITC-conjugated anti-CD45 (1 : 10; BD Pharmingen), FITC-conjugated anti-CD90 (1 : 200; BD Pharmingen), FITC-conjugated anti-CD105 (1 : 10; BioLegend, San Diego, CA, USA), and FITC-conjugated anti-CD166 (1 : 20; MBL, Aichi, Japan). Stained cells were analyzed by FACSCalibur or FACSVantage SE (BD Biosciences). Cell sorting was performed on a FACSVantage SE.

Cell culture. For adipogenic differentiation, sorted cells were cultured on Matrigel-coated (BD Biosciences) eight-well chamber slides (Nalge Nunc, Waltham, MA, USA) in GM at 37 °C in 5% CO_2 and 3% O_2. Ten thousands cells were plated per well. After 3 days, cells were treated with an adipogenic induction medium consisting of DMEM with 10% FBS, 0.5 mM IBMX (Sigma), 0.25 μM dexamethasone (Sigma), and 10 μg/ml insulin (Sigma) for 3 days,

Figure 5 Fibrogenic potential of PDGFRα^+ cells and effects of TGF-β and PDGF signaling on PDGFRα^+ cells. (**a**) Single PDGFRα^+ cell-derived colonies were stained with antibodies against collagen I (Col1) and FABP4 or FABP4 and α-smooth muscle actin (α-SMA). FABP4 antibody labeled adipocytes with lipid droplet, whereas Col1 and α-SMA were detected only in fibrogenic cells. Scale bar: 50 μm. (**b**) CD56$^+$ cells or PDGFRα^+ cells were cultured with or without TGF-β1 (5 ng/ml) for 3 days, and the expressions of fibrosis-related genes were quantified by quantitative real-time polymerase chain reaction (qRT-PCR). Values are represented as the ratio to unstimulated CD56$^+$ cells and shown as means ± s.d. of three independent preparations. *$P<0.01$, **$P<0.05$. (**c**) Western blot analysis of collagen I, collagen III, and glyceraldehyde 3-phosphate dehydrogenase (GAPDH). Results from two independent preparations were shown. (**d**) Matrix metalloproteinase (MMP) activity in the cell culture supernatants. Values are represented as the substrate amounts that were cleaved by MMPs contained in the supernatants and shown as means ± s.d. of three independent preparations. (**e**) Tissue inhibitors of metalloproteinase-1 (TIMP-1) concentration in the cell culture supernatants. Values are shown as means ± s.d. of three independent preparations. (**f**) PDGFRα^+ cells were cultured in SFM with or without PDGF-AA (10 ng/ml) for 2 days. Inhibitors were added 1 h before PDGF-AA stimulation. The extent of PDGFRα phosphorylation is represented as the ratio to unstimulated control cells (cont) and shown as means ± s.d. of three independent preparations. *$P<0.01$, **$P<0.05$. (**g**) Proliferation of PDGFRα^+ cells was quantified by measuring BrdU incorporation. Values are represented as the ratio to unstimulated control cells (cont) and shown as means ± s.d. of three independent preparations. *$P<0.01$; *versus* control culture. (**h** and **i**) PDGFRα^+ cells cultured in SFM were stimulated with PDGF-AA (10 ng/ml) for 15 min. Inhibitors were added 1 h before PDGF-AA stimulation. Phosphorylation of Akt and p44/42 MAPK was assessed by immunoblotting (**h**) and immunofluorescent staining (**i**). Scale bar: 50 μm in **i**

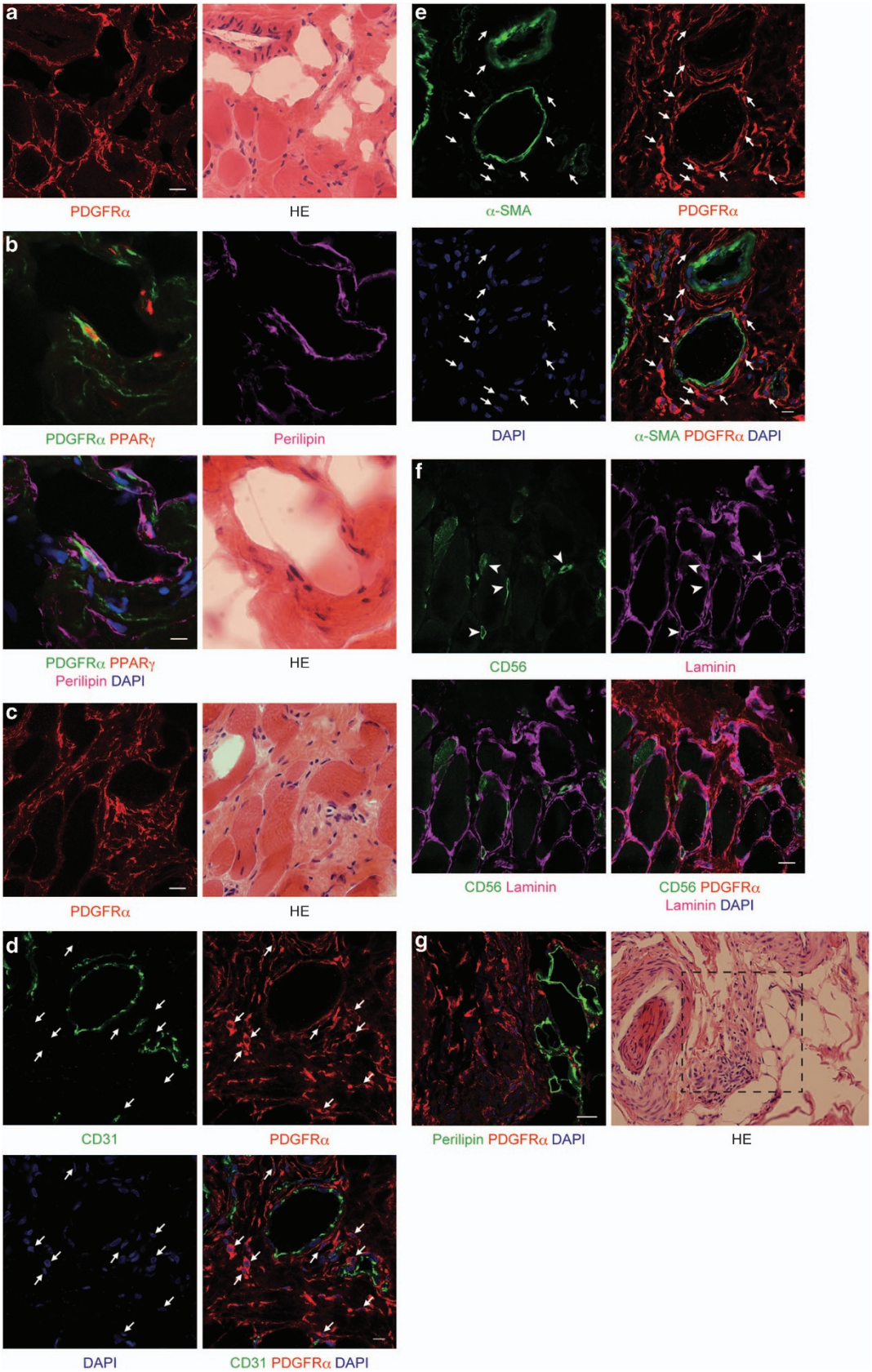
a
PDGFRα
HE
e
α-SMA
PDGFRα
b
PDGFRα PPARγ
Perilipin
DAPI
α-SMA PDGFRα DAPI
PDGFRα PPARγ
Perilipin DAPI
HE
f
CD56
Laminin
c
CD56 Laminin
CD56 PDGFRα
Laminin DAPI
PDGFRα
HE
d
g
CD31
PDGFRα
Perilipin PDGFRα DAPI
HE
DAPI
CD31 PDGFRα DAPI

followed by adipogenic maintenance medium consisting of DMEM with 10% FBS and 10 μg/ml insulin for 1 day at 37 °C in 5% CO_2 and 21% O_2. This treatment was repeated three times. For clonal analysis, sorted PDGFRα^+ cells were seeded onto a Matrigel-coated 96-well plate at a density of 0.8 cell per well and incubated for 7 days in GM at 37 °C in 5% CO_2 and 3% O_2. After 7 days, adipogenic induction was carried out as described above. For TGF-β1 stimulation, cells were cultured in 10% FBS-DMEM with or without 5 ng/ml TGF-β1 (R&D) for 3 days. For PDGF-AA stimulation, cells were serum-starved for 24 h by culturing in

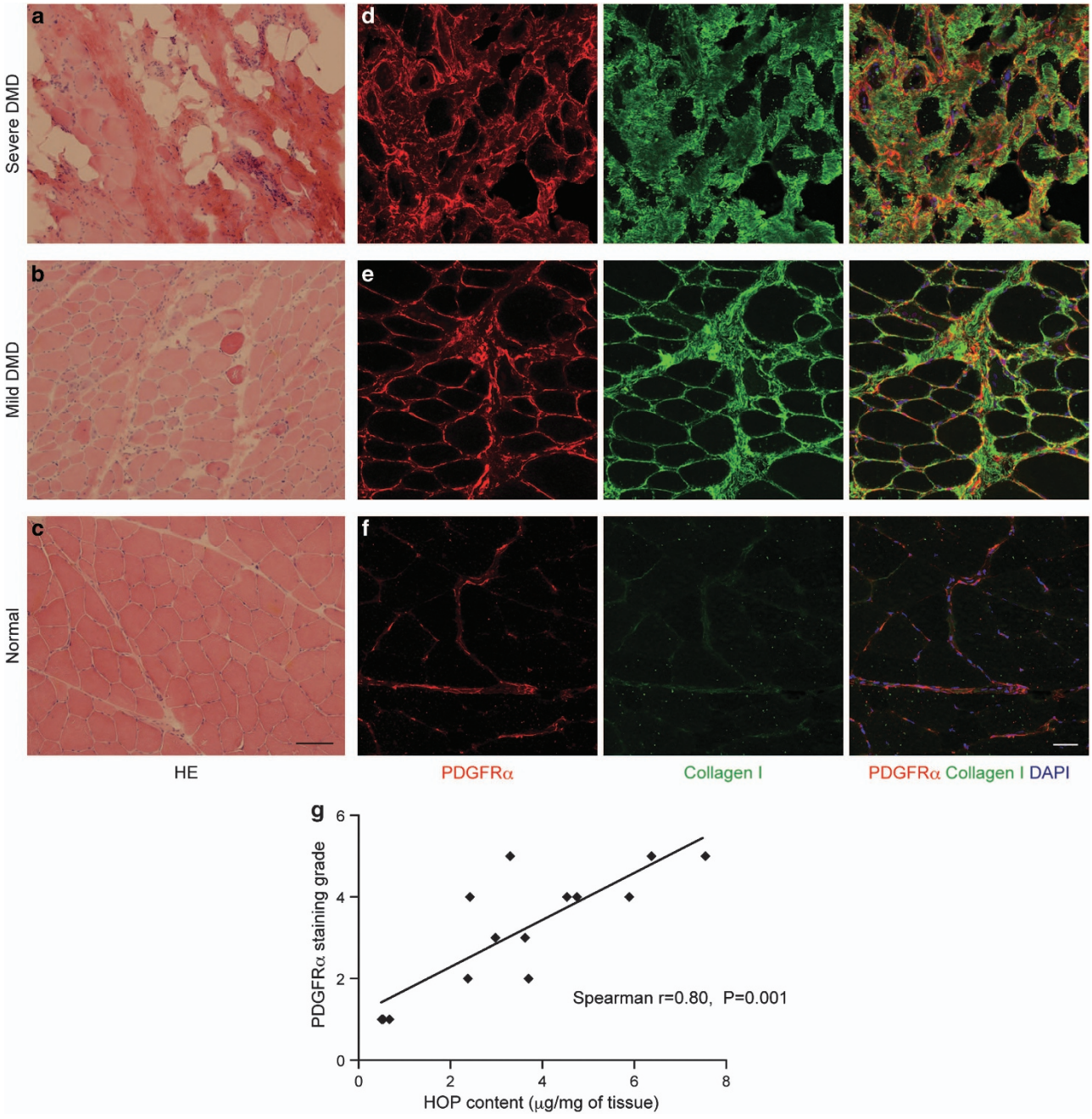

Figure 7 Correlation between the extent of PDGFRα staining and severity of fibrosis. (**a**–**c**) Muscle sections from DMD (**a** and **b**) and control (**c**) patients were subjected to HE staining. Scale bar: 100 μm. (**d**–**f**) Muscle sections from DMD (**d** and **e**) and control (**f**) patients were subjected to immunofluorescent staining for PDGFRα and collagen I. Scale bar: 20 μm. (**g**) PDGFRα staining grades correlate positively with severity of fibrosis (Spearman's rank correlation coefficient = 0.80, $P = 0.001$)

Figure 6 Pathological behavior of PDGFRα^+ cells in human diseased muscle. DMD muscle sections exhibiting fatty and fibrous degeneration were subjected to immunofluorescent staining for PDGFRα (**a** and **c**), or PDGFRα, peroxisome proliferator-activated receptor-γ (PPARγ), and perilipin (**b**), and subsequently to HE staining. DMD muscle sections were subjected to immunofluorescent staining for CD31 and PDGFRα (**d**), or α-smooth muscle actin (α-SMA) and PDGFRα (**e**). Arrows indicate PDGFRα^+ cells located around blood vessels. (**f**) DMD muscle sections were subjected to immunofluorescent staining for CD56, PDGFRα, and laminin. Arrowheads indicate CD56$^+$ cells located inside of the basement membrane. Volkmann's contracture muscle samples were subjected to immunofluorescent staining for PDGFRα and perilipin, and subsequently to HE staining (**g**). Fluorescent image corresponds to boxed area in HE image. Scale bars: 20 μm in (**a**, **c** and **g**), 10 μm in (**b**, **d**, **e** and **f**)

SFM consisting of DMEM supplemented with 2% Serum Replacement 1 reagent (Sigma). Then, cells were cultured in SFM with or without 10 ng/ml PDGF-AA (R&D) for 2 days. Imatinib (10 μM; Alexis, Farmingdale, NY, USA), anti-PDGFRα (5 μg/ml; R&D; cat. no. AF-307-NA), LY294002 (25 μM; Cell Signaling), PD98059 (50 μM; Cell Signaling), or U0126 (10 μM; Cell Signaling) were added 1 h before PDGF-AA stimulation. Cell viability was examined using ProstoBlue reagent (Invitrogen).

RNA extraction and RT-PCR. Total RNA was extracted using an RNeasy Micro Kit (Qiagen, Hilden, Germany), and equal amounts of RNA were reverse transcribed into cDNA using a QuantiTect Reverse Transcription Kit (Qiagen). The PCR reactions were performed with 0.5 μl cDNA product under the following cycling conditions: 94 °C for 30 s, followed by 30 cycles of amplification (94 °C for 5 s, 60 °C for 20 s, 72 °C for 10 s), and a final incubation at 72 °C for 5 min. Real-time quantitative PCR was performed on a Thermal Cycler Dice Real Time System (Takara, Shiga, Japan) with SYBR Premix Ex Taq (Takara) under the following cycling conditions: 95 °C for 10 s, followed by 40 cycles of amplification (95 °C for 5 s, 60 °C for 15 s, 72 °C for 10 s) and dissociation curve analysis. Specific primer sequences used in this study were: 5′-TGGCTTTCAACCATCTCATTC-3′ and 5′-GTGCTGCTGGGATCTGACAC-3′ for Pax3, 5′-GACCCCTGCCTAACCACATC-3′ and 5′-GTCTCCTGGTAGCGGCAAAG-3′ for Pax7, 5′-GAGGTGTACCACGACCA ACC-3′ and 5′-CCTGCTCTCTCAGCAACTCC-3′ for MYF5, 5′-GCCACAACGGAC GACTTCTATG-3′ and 5′-TGCTCTTCGGGTTTCAGGAG-3′ for MYOD1, 5′-TCCT CTGCCTGACATTGACC-3′ and 5′-TGAAGGTGGAACTGCTGGAAC-3′ for PDGFRA, 5′-AACCCTGTGCGGATTCTTG-3′ and 5′-GGAGACTGACTGCGTGTGTG-3′ for LEP, 5′-AAATCAGCTCCGCCTCTCTC-3′ and 5′-GGGTTGCCCAATGAATACTG-3′ for UCP1, 5′-GCAAGGTGTTGTGCGATGAC-3′ and 5′-TTGGTCGGTGGGTGACT CTG-3′ for COL1A1, 5′-AACCAGGAGCTAACGGTCTCA-3′ and 5′-CCAGGGTTT CCATCTCTTCC-3′ for COL3A1, 5′-CAATGGCTCTGGGCTCTGT-3′ and 5′-TGCT CTGTGCTTCGTCACC-3′ for ACTA2, and 5′-ACCCACTCCTCCACCTTTGA-3′ and 5′-TTGCTGTAGCCAAATTCGTTG-3′ for GAPDH.

Quantitative analyses of cell differentiation. To measure the extent of differentiation of cultured cells, five to seven randomly selected fields were photographed per well. Images were collected and pooled from three independent experiments. The percentage of positive cells was determined by dividing the number of marker$^+$ cells by the number of DAPI$^+$ nuclei using the Win ROOF software (Mitani Corp., Fukui, Japan). To assess the efficiency of adipogenic differentiation, Oil Red O-stained cells were extracted with 100 μl of 4% NP-40 in isopropanol for 5 min, and the absorbance of the dye–triglyceride complex was measured at 520 nm.

Immunoblot analysis. Cells were lysed in lysis buffer consisting of 50 mM Tris-HCl (pH 7.5), 150 mM NaCl, 1 mM NaF, 1% NP-40, and protease inhibitor cocktail (Roche, Basel, Switzerland). For the detection of phosphorylated proteins, lysis buffer was supplemented with phosphatase inhibitor cocktail (Roche). Cell lysates were centrifuged at 1000 $\times$ *g* for 10 min at 4 °C and the supernatants were recovered. Aliquots of the lysates containing 10 μg of protein were separated by sodium dodecyl sulfate-polyacrylamide gel electrophoresis and transferred onto polyvinylidene difluoride membranes. The membranes were probed with anti-collagen I (1 : 1000; Abcam), anti-collagen III (1 : 2000; Abcam), anti-GAPDH (1 : 2000; Cell Signaling), anti-phospho-Akt (1 : 2000; Cell Signaling), anti-Akt (1 : 1000; Cell Signaling), anti-phospho-p44/42 MAPK (1 : 2000; Cell Signaling), and anti-p44/42 MAPK (1 : 1000; Cell Signaling). After incubation with horseradish peroxidase-conjugated secondary antibodies and chemiluminescence reactions, images of the developed immunoblots were captured using a Light-Capture imaging system (Atto, Tokyo, Japan).

Measurement of MMP activity. TGF-β1 stimulation was carried out as described above. Cell supernatants were collected and centrifuged at 1000 $\times$ *g* for 10 min at 4 °C. The supernatants were recovered and MMP activity in the supernatants was measured by SensoLyte Generic MMP Fluorimetric Assay Kit (AnaSpec, Fremont, CA, USA).

Measurement of TIMP-1 concentration. TGF-β1 stimulation was carried out as described above. Cell supernatants were collected and centrifuged at 1000 $\times$ *g* for 10 min at 4 °C. The supernatants were recovered and TIMP-1 concentration in the supernatants was measured by Human TIMP-1 Quantikine ELISA Kit (R&D).

Measurement of PDGFRα phosphorylation. PDGFRα^+ cells were seeded onto 100 mm dishes. PDGF-AA stimulation was carried out as described above. Cells were rinsed with PBS two times and then lysed in 250 μl of lysis buffer consisting of 1% NP-40 Alternative, 20 mM Tris (pH 8.0), 137 mM NaCl, 10% glycerol, 2 mM EDTA, 1 mM activated sodium orthovanadate, 10 μg/ml aprotinin, and 10 μg/ml leupeptin for 15 min on ice. Samples were centrifuged at 10 000 $\times$ *g* for 5 min at 4 °C, and supernatants were recovered. Protein concentrations were quantified using DC protein assay (Bio-Rad, Hercules, CA, USA). PDGFRα phosphorylation was measured using equal amount of proteins by Human Phospho-PDGFRα DuoSet IC Kit (R&D).

Proliferation assay. PDGFRα^+ cells were seeded onto 96-well plate. PDGF-AA stimulation was carried out as described above. One day after adding PDGF-AA, 10 μM BrdU was added to each well. After 2 days stimulation, BrdU incorporation was measured using Cell Proliferation ELISA Kit (Roche).

HOP measurement. Frozen muscle tissues of 10–30 mg were homogenized in H_2O by Shakeman homogenizer (BMS, Tokyo, Japan) using 100 μl H_2O for every 10 mg of tissue. HOP content in the homogenates was measured using HOP Colorimetric Assay Kit (BioVision, Milpitas, CA, USA).

Statistics. Significance of the difference between two groups was assessed by Student's *t*-test. For comparisons of more than two groups, one-way analysis of variance (ANOVA) followed by Tukey's test or Dunnett's test was used for statistical analysis. To assess correlation between the extent of PDGFRα staining and severity of fibrosis, Spearman's rank correlation coefficient was used. A probability of $<5\%$ ($P<0.05$) was considered statistically significant.

Conflict of Interest

The authors declare no conflict of interest.

Acknowledgements. We thank K Ono for proofreading the paper. This work was supported by JSPS KAKENHI (24659687 and 24590363), Kato Memorial Bioscience Foundation, and The Nakatomi Foundation.

1. Bischof R. Satellite and stem cells in muscle regeneration. In: Engel AG, Franzini-Armstrong C (eds) *Myology*. 3rd edn. Vol. 1, McGraw-Hill: New York, NY, USA, 2004. pp 66–86.
2. Sherwood RI, Christensen JL, Conboy IM, Conboy MJ, Rando TA, Weissman IL *et al.* Isolation of adult mouse myogenic progenitors: functional heterogeneity of cells within and engrafting skeletal muscle. *Cell* 2004; **119**: 543–554.
3. Lepper C, Partridge TA, Fan CM. An absolute requirement for Pax7-positive satellite cells in acute injury-induced skeletal muscle regeneration. *Development* 2011; **138**: 3639–3646.
4. Sambasivan R, Yao R, Kissenpfennig A, Van Wittenberghe L, Paldi A, Gayraud-Morel B *et al.* Pax7-expressing satellite cells are indispensable for adult skeletal muscle regeneration. *Development* 2011; **138**: 3647–3656.
5. Collins CA, Olsen I, Zammit PS, Heslop L, Petrie A, Partridge TA *et al.* Stem cell function, self-renewal, and behavioral heterogeneity of cells from the adult muscle satellite cell niche. *Cell* 2005; **122**: 289–301.
6. Montarras D, Morgan J, Collins C, Relaix F, Zaffran S, Cumano A *et al.* Direct isolation of satellite cells for skeletal muscle regeneration. *Science* 2005; **309**: 2064–2067.
7. Sacco A, Doyonnas R, Kraft P, Vitorovic S, Blau HM. Self-renewal and expansion of single transplanted muscle stem cells. *Nature* 2008; **456**: 502–506.
8. Rocheteau P, Gayraud-Morel B, Siegl-Cachedenier I, Blasco MA, Tajbakhsh S. A subpopulation of adult skeletal muscle stem cells retains all template DNA strands after cell division. *Cell* 2012; **148**: 112–125.
9. Uezumi A, Fukada S, Yamamoto N, Takeda S, Tsuchida K. Mesenchymal progenitors distinct from satellite cells contribute to ectopic fat cell formation in skeletal muscle. *Nat Cell Biol* 2010; **12**: 143–152.
10. Uezumi A, Ito T, Morikawa D, Shimizu N, Yoneda T, Segawa M *et al.* Fibrosis and adipogenesis originate from a common mesenchymal progenitor in skeletal muscle. *J Cell Sci* 2011; **124**(Part 21): 3654–3664.
11. Joe AW, Yi L, Natarajan A, Le Grand F, So L, Wang J *et al.* Muscle injury activates resident fibro/adipogenic progenitors that facilitate myogenesis. *Nat Cell Biol* 2010; **12**: 153–163.
12. Starkey JD, Yamamoto M, Yamamoto S, Goldhamer DJ. Skeletal muscle satellite cells are committed to myogenesis and do not spontaneously adopt nonmyogenic fates. *J Histochem Cytochem* 2011; **59**: 33–46.
13. Irintchev A, Zeschnigk M, Starzinski-Powitz A, Wernig A. Expression pattern of M-cadherin in normal, denervated, and regenerating mouse muscles. *Dev Dyn* 1994; **199**: 326–337.

14. Seale P, Sabourin LA, Girgis-Gabardo A, Mansouri A, Gruss P, Rudnicki MA. Pax7 is required for the specification of myogenic satellite cells. *Cell* 2000; **102**: 777–786.
15. Sajko S, Kubinova L, Cvetko E, Kreft M, Wernig A, Erzen I. Frequency of M-cadherin-stained satellite cells declines in human muscles during aging. *J Histochem Cytochem* 2004; **52**: 179–185.
16. Reimann J, Brimah K, Schroder R, Wernig A, Beauchamp JR, Partridge TA. Pax7 distribution in human skeletal muscle biopsies and myogenic tissue cultures. *Cell Tissue Res* 2004; **315**: 233–242.
17. Verdijk LB, Koopman R, Schaart G, Meijer K, Savelberg HH, van Loon LJ. Satellite cell content is specifically reduced in type II skeletal muscle fibers in the elderly. *Am J Physiol Endocrinol Metab* 2007; **292**: E151–E157.
18. Lindstrom M, Thornell LE. New multiple labelling method for improved satellite cell identification in human muscle: application to a cohort of power-lifters and sedentary men. *Histochem Cell Biol* 2009; **132**: 141–157.
19. Capkovic KL, Stevenson S, Johnson MC, Thelen JJ, Cornelison DD. Neural cell adhesion molecule (NCAM) marks adult myogenic cells committed to differentiation. *Exp Cell Res* 2008; **314**: 1553–1565.
20. Schubert W, Zimmermann K, Cramer M, Starzinski-Powitz A. Lymphocyte antigen Leu-19 as a molecular marker of regeneration in human skeletal muscle. *Proc Natl Acad Sci USA* 1989; **86**: 307–311.
21. Illa I, Leon-Monzon M, Dalakas MC. Regenerating and denervated human muscle fibers and satellite cells express neural cell adhesion molecule recognized by monoclonal antibodies to natural killer cells. *Ann Neurol* 1992; **31**: 46–52.
22. Fidzianska A, Kaminska A. Neural cell adhesion molecule (N-CAM) as a marker of muscle tissue alternations. Review of the literature and own observations. *Folia Neuropathol* 1995; **33**: 125–128.
23. Webster C, Pavlath GK, Parks DR, Walsh FS, Blau HM. Isolation of human myoblasts with the fluorescence-activated cell sorter. *Exp Cell Res* 1988; **174**: 252–265.
24. Belles-Isles M, Roy R, Dansereau G, Goulet M, Roy B, Bouchard JP *et al.* Rapid selection of donor myoblast clones for muscular dystrophy therapy using cell surface expression of NCAM. *Eur J Histochem* 1993; **37**: 375–380.
25. Dellavalle A, Sampaolesi M, Tonlorenzi R, Tagliafico E, Sacchetti B, Perani L *et al.* Pericytes of human skeletal muscle are myogenic precursors distinct from satellite cells. *Nat Cell Biol* 2007; **9**: 255–267.
26. Pisani DF, Dechesne CA, Sacconi S, Delplace S, Belmonte N, Cochet O *et al.* Isolation of a highly myogenic CD34-negative subset of human skeletal muscle cells free of adipogenic potential. *Stem Cells* 2010; **28**: 753–764.
27. Pisani DF, Clement N, Loubat A, Plaisant M, Sacconi S, Kurzenne JY *et al.* Hierarchization of myogenic and adipogenic progenitors within human skeletal muscle. *Stem Cells* 2010; **28**: 2182–2194.
28. Lecourt S, Marolleau JP, Fromigue O, Vauchez K, Andriamanalijaona R, Ternaux B *et al.* Characterization of distinct mesenchymal-like cell populations from human skeletal muscle *in situ* and *in vitro*. *Exp Cell Res* 2010; **316**: 2513–2526.
29. Scott IC, Tomlinson W, Walding A, Isherwood B, Dougall IG. Large-scale isolation of human skeletal muscle satellite cells from post-mortem tissue and development of quantitative assays to evaluate modulators of myogenesis. *J Cachexia Sarcopenia Muscle* 2013; **4**: 157–169.
30. Vauchez K, Marolleau JP, Schmid M, Khattar P, Chapel A, Catelain C *et al.* Aldehyde dehydrogenase activity identifies a population of human skeletal muscle cells with high myogenic capacities. *Mol Ther* 2009; **17**: 1948–1958.
31. van Lochem EG, van der Velden VH, Wind HK, te Marvelde JG, Westerdaal NA, van Dongen JJ. Immunophenotypic differentiation patterns of normal hematopoiesis in human bone marrow: reference patterns for age-related changes and disease-induced shifts. *Cytometry B* 2004; **60**: 1–13.
32. Mackey AL, Kjaer M, Charifi N, Henriksson J, Bojsen-Moller J, Holm L *et al.* Assessment of satellite cell number and activity status in human skeletal muscle biopsies. *Muscle Nerve* 2009; **40**: 455–465.
33. Meng J, Adkin CF, Xu SW, Muntoni F, Morgan JE. Contribution of human muscle-derived cells to skeletal muscle regeneration in dystrophic host mice. *PLoS One* 2011; **6**: e17454.
34. Bruder SP, Ricalton NS, Boynton RE, Connolly TJ, Jaiswal N, Zaia J *et al.* Mesenchymal stem cell surface antigen SB-10 corresponds to activated leukocyte cell adhesion molecule and is involved in osteogenic differentiation. *J Bone Miner Res* 1998; **13**: 655–663.
35. Olson LE, Soriano P. Increased PDGFRalpha activation disrupts connective tissue development and drives systemic fibrosis. *Dev Cell* 2009; **16**: 303–313.
36. Andrae J, Gallini R, Betsholtz C. Role of platelet-derived growth factors in physiology and medicine. *Genes Dev* 2008; **22**: 1276–1312.
37. Heydemann A, Huber JM, Demonbreun A, Hadhazy M, McNally EM. Genetic background influences muscular dystrophy. *Neuromuscul Disord* 2005; **15**: 601–609.
38. Banker BQ, Engel AG. Basic reactions of muscle. In: Engel AG, Franzini-Armstrong C (eds) *Myology*. 3 edn. Vol. 1, McGraw-Hill: New York, NY, USA, 2004. pp 691–747.
39. Kragstrup TW, Kjaer M, Mackey AL. Structural, biochemical, cellular, and functional changes in skeletal muscle extracellular matrix with aging. *Scand J Med Sci Sports* 2011; **21**: 749–757.
40. Schulz TJ, Huang TL, Tran TT, Zhang H, Townsend KL, Shadrach JL *et al.* Identification of inducible brown adipocyte progenitors residing in skeletal muscle and white fat. *Proc Natl Acad Sci USA* 2011; **108**: 143–148.
41. Holmes C, Stanford WL. Concise review: stem cell antigen-1: expression, function, and enigma. *Stem Cells* 2007; **25**: 1339–1347.
42. Takashima Y, Era T, Nakao K, Kondo S, Kasuga M, Smith AG *et al.* Neuroepithelial cells supply an initial transient wave of MSC differentiation. *Cell* 2007; **129**: 1377–1388.
43. Morikawa S, Mabuchi Y, Kubota Y, Nagai Y, Niibe K, Hiratsu E *et al.* Prospective identification, isolation, and systemic transplantation of multipotent mesenchymal stem cells in murine bone marrow. *J Exp Med* 2009; **206**: 2483–2496.
44. Pinho S, Lacombe J, Hanoun M, Mizoguchi T, Bruns I, Kunisaki Y *et al.* PDGFRalpha and CD51 mark human nestin + sphere-forming mesenchymal stem cells capable of hematopoietic progenitor cell expansion. *J Exp Med* 2013; **210**: 1351–1367.
45. da Silva Meirelles L, Chagastelles PC, Nardi NB. Mesenchymal stem cells reside in virtually all post-natal organs and tissues. *J Cell Sci* 2006; **119**(Part 11): 2204–2213.
46. Crisan M, Yap S, Casteilla L, Chen CW, Corselli M, Park TS *et al.* A perivascular origin for mesenchymal stem cells in multiple human organs. *Cell Stem Cell* 2008; **3**: 301–313.
47. Soriano P. The PDGF alpha receptor is required for neural crest cell development and for normal patterning of the somites. *Development* 1997; **124**: 2691–2700.
48. Huang P, Zhao XS, Fields M, Ransohoff RM, Zhou L. Imatinib attenuates skeletal muscle dystrophy in mdx mice. *FASEB J* 2009; **23**: 2539–2548.
49. Bizario JC, Cerri DG, Rodrigues LC, Oliveira GL, Nomizo A, de Araujo DD *et al.* Imatinib mesylate ameliorates the dystrophic phenotype in exercised mdx mice. *J Neuroimmunol* 2009; **212**: 93–101.
50. Ito T, Ogawa R, Uezumi A, Ohtani T, Watanabe Y, Tsujikawa K *et al.* Imatinib attenuates severe mouse dystrophy and inhibits proliferation and fibrosis-marker expression in muscle mesenchymal progenitors. *Neuromuscul Disord* 2013; **23**: 349–356.
51. Ma LK, Li Q, He LF, Hua JS, Zhou JL, Yu H *et al.* Imatinib attenuates myocardial fibrosis in association with inhibition of the PDGFRalpha activity. *Arq Bras Cardiol* 2012; **99**: 1082–1091.
52. Wosczyna MN, Biswas AA, Cogswell CA, Goldhamer DJ. Multipotent progenitors resident in the skeletal muscle interstitium exhibit robust BMP-dependent osteogenic activity and mediate heterotopic ossification. *J Bone Miner Res* 2012; **27**: 1004–1017.
53. Oishi T, Uezumi A, Kanaji A, Yamamoto N, Yamaguchi A, Yamada H *et al.* Osteogenic differentiation capacity of human skeletal muscle-derived progenitor cells. *PLoS One* 2013; **8**: e56641.
54. Murphy MM, Lawson JA, Mathew SJ, Hutcheson DA, Kardon G. Satellite cells, connective tissue fibroblasts and their interactions are crucial for muscle regeneration. *Development* 2011; **138**: 3625–3637.

Cell Death and Disease **is an open-access journal published by** ***Nature Publishing Group*****. This work is licensed under a Creative Commons Attribution-NonCommercial-ShareAlike 3.0 Unported License. The images or other third party material in this article are included in the article's Creative Commons license, unless indicated otherwise in the credit line; if the material is not included under the Creative Commons license, users will need to obtain permission from the license holder to reproduce the material. To view a copy of this license, visit http://creativecommons.org/licenses/by-nc-sa/3.0/**

Supplementary Information accompanies this paper on Cell Death and Disease website (http://www.nature.com/cddis)